

Structure and Bonding of KSiH_3 and Its 18-Crown-6 Derivatives: Unusual Ambidentate Behavior of the $[\text{SiH}_3]^-$ Anion

David J. Wolstenholme,^{*,†} Paul D. Prince,[‡] G. Sean McGrady,^{*,†} Michael J. Landry,[†] and Jonathan W. Steed^{*,§}

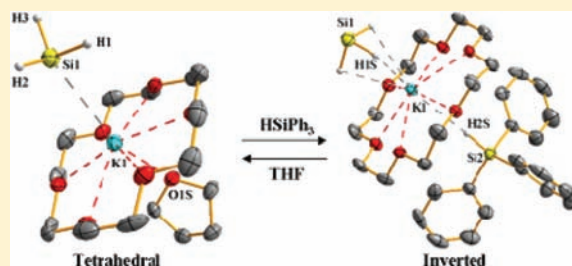
[†]Department of Chemistry, University of New Brunswick, P.O. Box 4400, Fredericton, New Brunswick E3B 5A3, Canada

[‡]Department of Chemistry, King's College London, Strand, London WC2R 2LS, United Kingdom

[§]Department of Chemistry, University of Durham, South Road, Durham DH1 3LE, United Kingdom

S Supporting Information

ABSTRACT: Density functional theory (DFT) calculations of $[\text{K}(18\text{-crown-6})\text{SiH}_3]$ (**1**) and KSiH_3 (**2**) have shown that both the classical *tet* and non-classical *inv* coordination modes of the $[\text{SiH}_3]^-$ anion to the K^+ ion are energetically accessible. Single-crystal X-ray structures of the *tet* and *inv* derivatives $[\text{K}(18\text{-crown-6})\text{SiH}_3 \cdot \text{THF}]$ (**1a**) and $[\text{K}(18\text{-crown-6})\text{SiH}_3 \cdot \text{HSiPh}_3]$ (**1b**) confirm this conclusion, showing that small changes in the coordination sphere of the metal are sufficient to alter the orientation of the anion. A topological analysis of the calculated electron densities for **1** and **2** reveals that the $\text{K} \cdots \text{Si}$ interaction in the *tet* conformer of **2** possesses a significant amount of covalent character. In contrast, the *inv* form of **2** displays primarily electrostatic character for the $\text{K} \cdots \text{Si}$ and $\text{K} \cdots \text{H}$ interactions. Incorporation of the 18-crown-6 ligand in **1** reduces the polarizing power of the K^+ cation, hardening the cation–anion interaction in both conformers. The experimental structures of **1a** and **1b** bear out these conclusions, with the strongly bound tetrahydrofuran (THF) ligand softening the K^+ ion in **1a** and favoring the *tet* conformer, while the weakly interacting HSiPh_3 ligand in **1b** has minimal effect on the K^+ center, resulting in an *inv* orientation.



INTRODUCTION

In contrast with the behavior of C–H bonds that constitute the passive framework of most organic molecules and materials, the difference in electronegativity between carbon and silicon (2.5 vs 1.8; cf. hydrogen 2.1),¹ in tandem with the significantly weaker Si–H bond (76 vs 98 kcal/mol),² conspire to endow the hydridic Si–H moiety with a chemical umpolung (polarity inversion) and enhanced reactivity. The bonding motifs exhibited by alkali metal silyl hydrides (MSiH_3) are also quite different from their organic counterparts, since these systems can adopt either a “classical” tetrahedral (*tet*) or “non-classical” inverted (*inv*) anion-to-cation orientation. The simplest MSiH_3 ($\text{M} = \text{K}, \text{Rb},$ and Cs) salts crystallize in the rock salt lattice ($Fm\bar{3}m$).^{3,4} However, poorly defined hydrogen atom positions and the crystallographic symmetry of this lattice conspire to prevent explicit assignment of a *tet* or *inv* geometry. Conversely, a number of alkali metal tris(trimethylsilyl)silanide complexes have been shown to crystallize as dimers that exhibit pseudo tetrahedral coordination of the $\text{Si}(\text{Me}_3\text{Si})_3$ moieties.⁵ In light of these issues, deeper insights into the structural proclivities of MSiH_3 complexes are needed to augment our limited understanding of the coordination chemistry of this intriguing class of inorganic systems.

Some 25 years ago, ab initio calculations by Schleyer and Clark predicted the *inv* structure of LiSiH_3 to be more stable than its *tet* counterpart ($\Delta E = E_{\text{inv}} - E_{\text{tet}} = -2.4$ kcal/mol).⁷ These authors

attributed the added stability of this unusual conformation to the presence of significant negative charge on the hydrogen atoms, resulting in strong electrostatic interactions with the Li^+ ions.⁷ In contrast, density functional theory (DFT) calculations by Pacios et al. have shown that NaSiH_3 adopts a *tet* geometry ($\Delta E = +2.4$ kcal/mol), notwithstanding the possibility of similar inter-ion interactions.^{8,9} The difference in the coordination modes of these two MSiH_3 complexes was believed to result from the much shorter anion-to-cation distances in the Li derivative, which maximizes the ionic effects.⁹ However, a more detailed analysis of the factors that underlie the geometry adopted by these MSiH_3 systems was not undertaken.

In spite of the early predictions of Schleyer and Clark, only a single well-defined MSiH_3 crystal structure has been reported in the Cambridge Structural Database (CSD). In this instance, the $[\text{SiH}_3]^-$ moiety of an oligomeric sodium alcoholate (HAZCUG) displays an *inv* orientation of the anion.⁶ This dearth of experimental structural data has restricted our understanding of the chemical bonding in metal silyl hydrides to theoretical modeling. In light of the underdeveloped and poorly understood coordination chemistry of these important main group systems, we have carried out a detailed experimental and theoretical study of the structure and bonding displayed by $[\text{K}(18\text{-crown-6})\text{SiH}_3]$ (**1**)

Received: August 15, 2011

Published: October 07, 2011

and its derivatives, along with a comparison with its parent compound KSiH_3 (**2**). We find that ΔE for both **1** and **2** is remarkably small, and that subtle changes in the local chemical environment of the K^+ ion in **1** can switch the $[\text{SiH}_3]^-$ coordination mode from *tet* to *inv*.¹⁰ We have also carried out an analysis of the electron distribution for these benchmark systems, which has assisted our understanding of the behavior of the $[\text{SiH}_3]^-$ anion. Our aim was to identify the factors that underlie the preference for a *tet* or *inv* coordination, and hence to obtain a deeper understanding of this fundamental area of main group structural chemistry.

RESULTS AND DISCUSSION

A recent MP2/6-31+G* study predicted the *tet* geometry to be the more stable orientation of the anion in KSiH_3 (**2**) ($\Delta E = +1.3$ kcal/mol).¹¹ However, our high level calculations (see Supporting Information) indicate that the *inv* form represents the ground state geometry of this system, although the two conformers are almost degenerate ($\Delta E = -0.3$ kcal/mol). In a similar fashion, coordination of the K^+ ion in **1** by the 18-crown-6 ligand results in two energy minima, with a marginal preference for the *inv* conformation ($\Delta E = -0.9$ kcal/mol). This feature is also apparent in the NMR spectra of **1a** and **1b**, in which the $[\text{SiH}_3]^-$ anion environment is almost identical, pointing to a low energy barrier between the two conformations. The almost identical energies associated with these coordination modes in **1** and **2** makes these systems ideal testbeds for exploring the factors that contribute to the structures adopted by MSiH_3 compounds.

Solid-State Structures of $[\text{K}(18\text{-crown-6})\text{SiH}_3 \cdot \text{THF}]$ (1a**) and $[\text{K}(18\text{-crown-6})\text{SiH}_3 \cdot \text{HSiPh}_3]$ (**1b**).** The single crystal structure of $[\text{K}(18\text{-crown-6})\text{SiH}_3 \cdot \text{THF}]$ (**1a**) reveals a *tet* orientation of the $[\text{SiH}_3]^-$ moiety, with the ancillary tetrahydrofuran (THF) ligand occupying a position *trans* to this anion (Figure 1a). This neutral ligand binds to K^+ with a comparable strength as the oxygen donors of the crown ether moiety ($d_{\text{K} \cdots \text{O}} = 2.835(3)$ Å for THF versus 2.805(3)–2.911(2) Å for 18-crown-6). The K^+ ion is situated 0.39 Å above the mean plane of the crown ether ligand and faces a *tet* $[\text{SiH}_3]^-$ moiety canted about 12° from the normal. The $\text{K} \cdots \text{Si}$ distance (3.592(1) Å) in **1a** is slightly longer than in its *inv* counterpart, $[\text{K}(18\text{-crown-6})\text{SiH}_3 \cdot \text{HSiPh}_3]$ (**1b**) (3.515(2) Å), consistent with the *inv* coordination of the $[\text{SiH}_3]^-$ anion reported for HAZCUG and NaSiH_3 complexes.⁶ In a similar vein, the calculated $\text{K} \cdots \text{Si}$ bonds in the *inv* form of **2** is also shorter than its *tet* counterpart. However, the optimized structure of **1**, which contains no ancillary ligand, displays essentially identical $\text{K} \cdots \text{Si}$ distances for both orientations of the anion (see Supporting Information).

In contrast, the solid-state structure of $[\text{K}(18\text{-crown-6})\text{SiH}_3 \cdot \text{HSiPh}_3]$ (**1b**) reveals a $[\text{K}(18\text{-crown-6})]^+$ moiety with the metal displaced 0.65 Å (cf. 0.39 Å in **1a**) above the mean plane of the crown ether toward an *inv* $[\text{SiH}_3]^-$ moiety (Figure 1b). The ancillary HSiPh_3 ligand again occupies the available site *trans* to this anion. The $\text{K} \cdots \text{H} \cdots \text{Si}$ distance (3.16 Å) for the HSiPh_3 ligand in **1b** invites comparison with that reported for the related hypervalent silicon hydride system $[\text{K}(18\text{-crown-6})][\text{H}_2\text{SiPh}_3]$,¹² in which the $\text{K} \cdots \text{H}$ distance is $\sim 15\%$ shorter (2.69 Å). We conclude that the ancillary HSiPh_3 moiety in **1b** exerts little influence on the local chemical environment of the K^+ ion, in contrast to the strongly bound THF ligand in **1a**, which draws the cation back toward the plane of the crown ether ligand by some 0.26 Å. The three subcomponents in **1b** share a common 3-fold

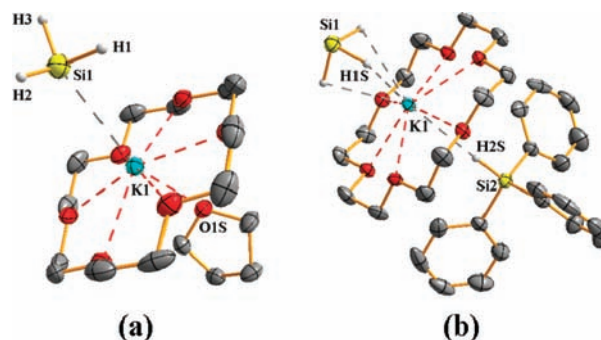


Figure 1. Single-crystal X-ray diffraction structures of (a) **1a** and (b) **1b**, with thermal ellipsoids at 50% probability. Salient bond lengths (Å) and angles (deg) are as follows: **1a**: $\text{K}(1) \cdots \text{Si}(1)$ 3.592(1); $\text{K}(1) \cdots \text{O}(1\text{S})$ 2.835(3); $\text{Si}(1) \cdots \text{H}(1)$ 1.55; $\text{Si}(1) \cdots \text{H}(2)$ 1.25; $\text{Si}(1) \cdots \text{H}(3)$ 1.43; $\text{Si}(1) - \text{K}(1) - \text{O}(1\text{S})$ 160.95(6). **1b**: $\text{K}(1) \cdots \text{Si}(1)$ 3.515(2); $\text{K}(1) \cdots \text{H}(1\text{S})$ 2.99; $\text{K}(1) \cdots \text{H}(2\text{S})$ 3.16; $\text{Si}(1) - \text{H}(1\text{S})$ 1.49; $\text{Si}(2) - \text{H}(2\text{S})$ 1.39; $\text{Si}(1) - \text{K}(1) - \text{Si}(2)$ 180.0.

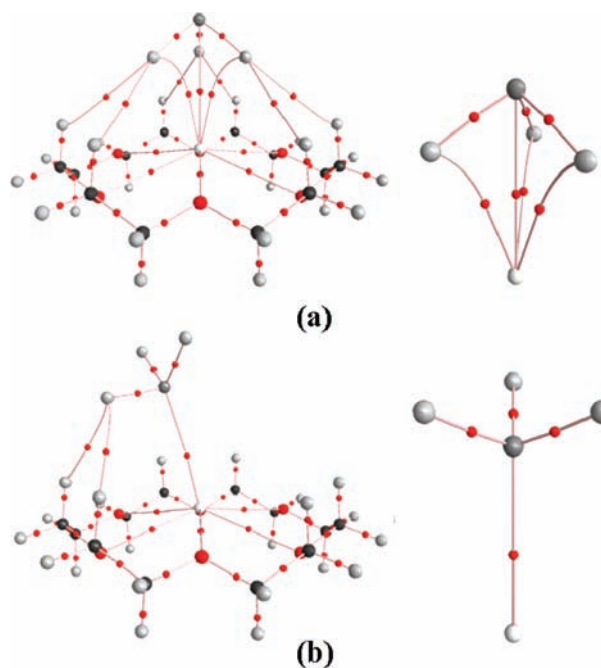


Figure 2. Complete set of bond paths for (a) *inv* and (b) *tet* forms of **1** and **2**. The bond critical points (BCP) are represented by small solid red circles.

axis and mirror plane defined by the rhombohedral space group $R3m:r$ ($Z' = 1/6$), with the axis extending along the $\text{Ph}_3\text{Si}-\text{H} \cdots \text{K} \cdots \text{SiH}_3$ directrix. The most prominent features of this structure are the $\text{K} \cdots \text{Si}$ and $\text{K} \cdots \text{H}$ distances (3.515(2) and 2.99 Å, respectively), which define the *inv* orientation of the ion pair.

Bonding in $[\text{K}(18\text{-crown-6})\text{SiH}_3]$ (1**) and KSiH_3 (**2**).** In an attempt to gain insight into the versatile chemical bonding displayed by these MSiH_3 complexes, we have analyzed the electron distribution in the *tet* and *inv* isomers of **1** and **2** according to the concepts developed in the theory of “Atoms in Molecules” (AIM).¹³ The molecular graphs for the *inv* structures reveal both $\text{K} \cdots \text{Si}$ and $\text{K} \cdots \text{H}$ interactions (Figure 2a), consistent with the bonding motif exhibited by the *inv* form of NaSiH_3 .⁹ In these instances, the electron density

Table 1. Topological Properties of the Calculated Electron Density for the Optimized *tet* and *inv* Structures of 1 and 2

compound	parameter	tetrahedral			inverted		
		d (Å)	$\rho_b(r)$ ($e \text{ \AA}^{-3}$)	$\nabla^2 \rho_b(r)$ ($e \text{ \AA}^{-5}$)	d (Å)	$\rho_b(r)$ ($e \text{ \AA}^{-3}$)	$\nabla^2 \rho_b(r)$ ($e \text{ \AA}^{-5}$)
1	Si–H	1.543	0.676	3.976	1.560	0.655	3.513
	Si–H	1.526	0.708	4.249	1.560	0.655	3.505
	Si–H	1.524	0.711	4.279	1.560	0.655	3.514
	K \cdots Si	3.329	0.099	0.747	3.334	0.073	0.842
	K \cdots H				2.784	0.073	0.837
	K \cdots H				2.782	0.073	0.838
	K \cdots H				2.782	0.073	0.838
	H \cdots H	2.556	0.034	0.305	2.857	0.020	0.181
	H \cdots H	2.547	0.034	0.310	2.861	0.020	1.180
	H \cdots H				2.888	0.019	0.173
	H \cdots H				2.886	0.019	0.173
	H \cdots H				2.870	0.020	0.178
	H \cdots H				2.866	0.020	0.179
	2	Si–H	1.512	0.733	4.601	1.565	0.653
K \cdots Si		3.162	0.143	0.921	3.111	0.107	1.221
K \cdots H					2.576	0.110	1.219

accumulated at the bond critical points (BCP), $\rho_b(r)$, for both the K \cdots Si and K \cdots H interactions turn out to be nearly identical, indicating that the electron density in the vicinity of the anion–cation interface is flat and delocalized (Table 1). This feature indicates that the $[\text{SiH}_3]^-$ moieties interact globally with the K $^+$ ions, in an analogous manner as the $[\text{BH}_4]^-$ anions in $[\text{Na}(15\text{-crown-5})\text{BH}_4]$ and $[\text{K}(18\text{-crown-6})\text{BH}_4]$.^{14,15} In contrast, the *tet* structures of 1 and 2 display a single K \cdots Si bond path between the cation and the anion (Figure 2b). The $\rho_b(r)$ values for the K \cdots Si interactions in this conformation are considerably larger than those of their *inv* counterparts, revealing a stronger interaction between the K and Si atoms.

The presence of the 18-crown-6 ligand in the *inv* and *tet* structures of 1 results in the formation of a number of weak inter-ion Si–H \cdots H–C interactions, which may be described as unconventional dihydrogen bonds between the hydridic Si–H bonds and the hydrogen bond donor $-\text{OCH}_2$.^{16–18} The Si–H bonds in the *inv* conformation of 1 each engage in bifurcated Si–H \cdots H–C interactions with the crown ether, while the *tet* conformer displays only two such interactions, with a unique Si–H bond. These weak interactions provide a possible explanation for the canting of the anion, a feature which is reproduced in the crystal structure of 1a, albeit less pronounced. It is noteworthy that similar Si–H \cdots H–C interactions were also identified in the solid-state structure of $[\text{K}(18\text{-crown-6})][\text{H}_2\text{SiPh}_3]$.¹² The charge redistribution within 2 attendant on coordination of the crown ether ligand to form 1 leads to a weakening of the primary inter-ion interactions in both the *tet* and *inv* conformers, as reflected in their distinctly smaller $\rho_b(r)$ values. The geometry adopted by the $[\text{SiH}_3]^-$ moiety thus appears to be controlled by different factors in KSiH_3 and in its crown ether adducts.

Secondary Interactions in $[\text{K}(18\text{-crown-6})\text{-SiH}_3 \cdot \text{THF}]$ (1a) and $[\text{K}(18\text{-crown-6})\text{SiH}_3 \cdot \text{HSiPh}_3]$ (1b). The driving force behind the preference of a *tet* or *inv* orientation for the $[\text{SiH}_3]^-$ moiety in the solid-state remains unclear, on account of only a handful of reported experimental and theoretical structures. However, it is clear that the intermolecular interactions which

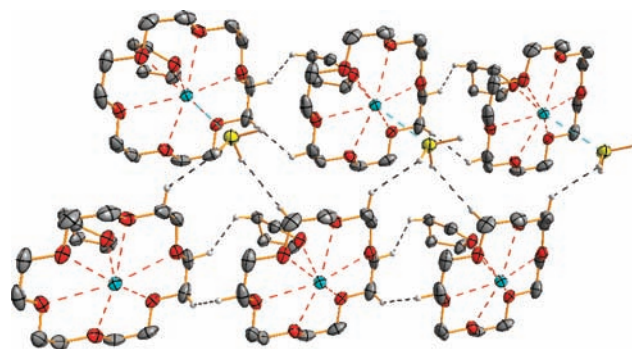


Figure 3. Extended structure of 1a, highlighting Si–H \cdots H–C and C–H \cdots H–C interactions between adjacent ion pairs. Salient bond lengths (Å) and angles (deg) are as follows: Si–H \cdots H–C = 2.46–2.69; Si–H \cdots H = 111–127; H \cdots H–C = 137–155; Si–H \cdots H–C = 13–68; C–H \cdots H–C = 2.33; C–H \cdots H = 150; H \cdots H–C = 116; Si–H \cdots H–C = 68; C–H \cdots H–C = 2.35; C–H \cdots H = 138; H \cdots H–C = 124; Si–H \cdots H–C = -166 . (see Supporting Information for further details).

stabilize the extended structures of these systems will play a role in determining whether a *tet* or *inv* geometry is adopted. Accordingly, we have explored the supramolecular chemistry of these MSiH_3 complexes 1a and 1b, which differ in the orientation of the $[\text{SiH}_3]^-$ anion as a result of small changes in the local coordination environment of the K $^+$ ions (i.e., the presence of different neutral ancillary ligands).

The Si–H bonds of the anion in 1a each engage in weak intermolecular Si–H \cdots H–C interactions with a methylene hydrogen atom of an adjacent crown ether ligand (Figure 3). These interactions are characterized by H \cdots H contacts ranging from 2.46 to 2.69 Å, which exceed the sum of the van der Waals radii for two interacting neutral hydrogen atoms (2.4 Å).¹⁹ However, the hydridic nature of the Si–H moieties increases the effective size of the hydrogen atom to about 1.39 Å, making 2.59 Å a more appropriate upper limit for identifying Si–H \cdots H–C

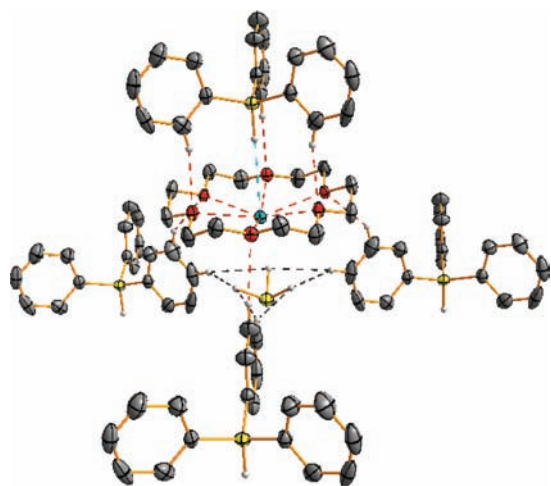


Figure 4. Extended structure of **1b**, highlighting the supramolecular Si–H···H–C and C–H···O interactions. Salient bond lengths (Å) and angles (deg) are as follows. Si–H···H–C = 2.55; Si–H···H = 91; H···H–C = 152; Si–H···H–C = –116; C–H···O = 2.50; C–H···O = 165; C–H···O = 2.62; C–H···O = 148.

Table 2. Theoretical Delocalization Indices (δ) for the *tet* and *inv* Forms of **1** and **2**

compound	tetrahedral		inverted	
	parameter	δ	parameter	δ
1	Si–H	0.685	Si–H	0.657
	Si–H	0.701	Si–H	0.658
	Si–H	0.700	Si–H	0.657
	K···Si	0.167	K···Si	0.057
	K···H		K···H	0.052
	K···H		K···H	0.052
	K···H		K···H	0.052
	H···H	0.027	H···H	0.016
	H···H	0.027	H···H	0.016
	H···H		H···H	0.015
	H···H		H···H	0.015
2	Si–H	0.700	Si–H	0.650
	K···Si	0.410	K···Si	0.157
	K···H		K···H	0.103

interactions.^{20,21} In contrast, the Si–H moieties in **1b** form bifurcated Si–H···H–C interactions with the para-H atoms of the phenyl groups of HSiPh₃ (Figure 4). The crystallographic symmetry of the *R3m* space group results in a single unique Si–H···H–C interaction, and the H···H distance for this contact is 2.55 Å, which once again falls at the upper limit identified for this type of interaction. The inter-ion Si–H···H–C interactions present in these two systems (vide supra) are characterized by experimental H···H distances greater than those of their supramolecular counterparts (2.87 Å in **1a** and 3.23 Å in **1b**), which highlights the role that the intermolecular interactions play in stabilizing the structure and geometry of these metal hydrides.

Table 3. Theoretical Atomic Charges (q) for the *tet* and *inv* Forms of **1** and **2**

compound	tetrahedral		inverted	
	atom	q	atom	q
1	K	0.862	K	0.878
	Si	1.265	Si	1.247
	H	–0.712	H	–0.709
	H	–0.707	H	–0.709
2	K	0.736	K	0.817
	Si	1.353	Si	1.316
	H	–0.696	H	–0.711

The crystal packing displayed by these MSiH₃ complexes reveals additional supramolecular interactions. Several close C–H···H–C contacts (2.33 and 2.35 Å) between the methylene hydrogen atoms of the THF and/or the crown ether in **1a** result in favorable electrostatic interactions, commonly referred to as H–H bonding.²² These H–H bonds connect adjacent crown ether molecules, and together with the Si–H···H–C dihydrogen interactions described above, effectively extending the structure in three dimensions. In contrast, the oxygen atoms of the crown ether in **1b** are involved in more conventional C–H···O hydrogen bonds, which appear to be solely responsible for the supramolecular architecture adopted by this system. Overall, the weak C–H···H–C and C–H···O interactions in these systems appear to play no role in directing the orientation of the [SiH₃][–] moieties, since these interactions do not directly involve the anions.

Hard–Soft Interactions in [K(18-crown-6)SiH₃] (1**) and KSiH₃ (**2**).** Although the geometry and topological analysis of the electron density presented above for **1** and **2** provides fundamental insights into the chemical bonding in these MSiH₃ systems, they reveal scant clues as to the controlling factors that determine whether a *tet* or *inv* geometry is adopted. The delocalization index, $\delta(A,B)$, which measures the number of electron pairs shared between two atoms, provides an alternative means of interpreting their chemical bonding.²³ A large δ value for the K···Si interaction in the *tet* structure of **2** (Table 2) implies a certain degree of covalent character associated with the inter-ion bonding in this system. Conversely, the K···Si and K···H interactions in the related *inv* form are characterized by smaller δ values, consistent with primarily electrostatic stabilization of the ion pair. It is noteworthy that the sum of the individual K···Si and K···H interactions contributes approximately the same amount to the overall stabilization of the *inv* complex as does the single K···Si interaction in its *tet* counterpart.

In terms of Pearson's hard–soft (Lewis) acid–base (HSAB) Principle,^{24,25} the anion-to-cation bonding in the *inv* form of **2** (consisting of both K···Si and K···H contributions) is a chemically harder interaction than is the more covalent (softer) K···Si interaction in the *tet* version of **2**. This conclusion is supported by an analysis of the atomic charges for these systems (Table 3). The K⁺ ion in the *inv* conformer of **2** is significantly more electron deficient than is the cation in its *tet* counterpart, and interacts preferentially with the more negatively charged face of the ambidentate [SiH₃][–] anion, through electrostatic K···H and K···Si interactions. In contrast, the somewhat less

electron-deficient K^+ ion in the *tet* structure of **2** interacts with the less negative portion of the anion through a single $K \cdots Si$ interaction. Hence, the geometry adopted by **2** appears to be strongly correlated with the hard or soft nature of the metal center to which the anion coordinates. This feature directly controls the amount of covalent character present in the $K \cdots Si$ bonds, with a *tet* structure being preferentially adopted as the covalency of this interaction increases.

The bonding scenario in the crown ether adducts is somewhat more complicated, since the coordinating oxygen atoms lower the positive charge on the K^+ ion, reducing its polarizing power and weakening its interaction with the $[SiH_3]^-$ moiety. Accordingly, the δ values for the $K \cdots Si$ and/or $K \cdots H$ interactions are considerably smaller than in the isolated parent species **2** (Table 2), resulting in the primary inter-ion interactions for both conformations of **1** being largely electrostatic in nature. The reduced polarizing power of the cation results in a chemically harder interaction between the K and Si atoms (Table 3). This feature is also revealed in the crystal structure of **1a**, where the THF donor ligand results in less charge transfer occurring between K^+ and $[SiH_3]^-$, giving rise to a softer anion-to-cation interaction and a more stable *tet* geometry. The electrostatic bonding between K^+ and $[SiH_3]^-$ in both conformers of **1** indicates a shift in the behavior of these two coordination modes toward a common bonding motif. However, the inter-ion and supramolecular $Si-H \cdots H-C$ interactions appear also to play a role in stabilizing these $MSiH_3$ complexes. The sum of the δ values for the bifurcated $Si-H \cdots H-C$ interactions in the *inv* structure of **1** is greater than the analogous contribution from the corresponding interactions in the *tet* isomer, a feature which serves to stabilize further the *inv* geometry. We conclude that the experimental and theoretical geometries adopted by the *tet* and *inv* crown ether adducts of **1** are determined by the interplay of several factors, including the electronic character of the metal binding site, the ambidentate nature of the $[SiH_3]^-$ anion, and the formation of non-classical inter-ion and supramolecular $Si-H \cdots H-C$ interactions with the crown ether moiety.

SUMMARY

DFT calculations for **1** and **2** indicate that the classical *tet* and non-classical *inv* coordination modes of the $[SiH_3]^-$ anion are both energetically accessible. This conclusion is borne out by the single crystal X-ray structures of **1a** and **1b**, which highlight that small changes in the local coordination environment of the metal center can reverse the orientation of the anion. A topological analysis of the electron distribution for these systems has provided insight into the features that dictate the preference of a *tet* or *inv* geometry. The *tet* structure of **2** is stabilized by a considerable degree of covalent character associated with the $K \cdots Si$ interaction, whereas the $K \cdots Si$ and $K \cdots H$ interactions for the *inv* conformation are predominantly electrostatic in nature, resulting in a global interaction of the $[SiH_3]^-$ moiety with the K^+ ion. Incorporation of the 18-crown-6 ligand in **1** reduces the polarizing power of the cation, causing the anion-to-cation interactions in both conformers to become more electrostatic in nature. The $[SiH_3]^-$ moiety hence behaves in a similar manner as established ambidentate anions such as NO_2^- and SCN^- , whose coordination modes are dictated by the hard or soft character of the metal binding site.² The presence of weak inter-ion and supramolecular $Si-H \cdots H-C$ interactions in the solid-state structure of the crown ether adducts **1a** and **1b**

provides an additional impetus for the $[SiH_3]^-$ anion to orient in certain conformation.

EXPERIMENTAL DETAILS

General Considerations. All manipulations were carried out under an inert atmosphere in either a nitrogen-filled glovebox or using an argon Schlenk line. The KH used throughout was purchased from Sigma Aldrich as a 60% suspension in mineral oil, which was transferred directly to a flask fitted with a Young's valve under an argon atmosphere. The mineral oil was then removed by washing with several portions of pentane, removing each aliquot in turn by cannula. The 18-crown-6 was dissolved in a minimum quantity of dry degassed Et_2O and stored over predried molecular sieves (4 Å) for at least 24 h. This solution was decanted from the sieves, and the solvent removed under reduced pressure. The dried KH and 18-crown-6 were each stored in the glovebox. Other reagents were purchased from commercial sources and used without further purification. Solvents were purified and dried by distillation from sodium metal using benzophenone as an indicator, and degassed by sparging with argon for 15–20 min. THF- d_8 was purchased from Goss and stored over sodium metal for a period of 2–3 d, followed by degassing using a freeze–pump–thaw method. The THF- d_8 was then decanted and stored over fresh sodium or predried molecular sieves (4 Å).

Synthesis and Characterization of $[K(18\text{-crown-6})SiH_3]$ (1**).** *Method 1.* Potassium metal (0.11 g, 2.56 mmol) was cut into small chunks (2 mm³) and placed in a Schlenk vessel. In a separate Schlenk, 18-crown-6 (0.69 g, 2.61 mmol) was dissolved in THF (30 mL), and the resulting solution was transferred via cannula onto the potassium with constant stirring. The metal dissolved gradually to give an intense blue solution. Gaseous SiH_4 , generated in situ by the reaction of $Si(OEt)_4$ with $LiAlH_4$ in nBu_2O , was transferred into the reaction vessel under a constant stream of N_2 , which acted as a carrier gas, and condensed onto the walls of the reaction vessel, which was maintained at $-196^\circ C$. The frozen solution of potassium and 18-crown-6 in DME was cautiously allowed to warm to ambient temperature with swirling, resulting in a color change from blue through colorless to yellow, and finally to amber (the surface of the metal changed from blue through gold to green). The mixture became cloudy after 1 h, and was left to stir for 24 h at room temperature. After standing for approximately 5 d, the mixture had separated into an off-white precipitate and a deep yellow colored solution. The 1H NMR spectrum of the white precipitate was consistent with $[K(18\text{-crown-6})SiH_3]$ (**1**). In addition, trace amounts of a hypervalent product were also observed from this reaction, which we have tentatively assigned as $[K(18\text{-crown-6})(p\text{-MeC}_6\text{H}_4)_3SiH_2]$. Diffraction quality crystals were obtained by dissolving this product in the minimum amount of warm THF, followed by layering with cold pentane.

1H NMR δ (THF- d_8): 1.2 (s, $^1J(^{29}Si-H) = 73.64$ Hz, 3H), 3.62 (s, 36H). ^{13}C NMR δ (THF- d_8): 70.57 (s, CH_2). ^{29}Si NMR δ (THF- d_8): -169.4 (q, $^1J(^{29}Si-H) = 73.66$ Hz. $^{29}Si\{^1H\}$ NMR δ (THF- d_8): -169.4 (s).

*Crystal Data for **1a** at 120(2) K (CCDC = 821709).* $M_r = 406.63$, with $Mo_{K\alpha}$ radiation (0.71073 Å); monoclinic space group Cc (no. 9), $a = 13.8625(8)$, $b = 10.0064(8)$, $c = 16.7283(10)$ Å, $\beta = 106.967(4)^\circ$, $V = 2219.4(3)$ Å³, $Z = 4$, $2\theta_{max} = 50.0^\circ$, 3697 unique reflections [$R_{int} = 0.0823$], $\mu = 0.323$ mm⁻¹, GOF = 1.008, $R1$ ($I > 2\sigma$) = 0.0409, $wR2$ (all data) = 0.0754, largest diff. peak and hole 0.245 and -0.325 e Å⁻³.

Method 2. Potassium metal (0.18 g, 4.62 mmol) cut into chunks (2–3 mm³) and placed in a Schlenk vessel. 18-crown-6 (1.22 g, 4.66 mmol) was dissolved in THF (45 mL) in a separate vessel and added to the potassium via cannula while stirring to give an intense blue colored solution. $PhSiH_3$ (1.7 mL, 1.49 g, 15.74 mmol) was then added to the reaction vessel via syringe, resulting in the same color changes as observed using method 1. After standing for 2 d, colorless crystals had

formed, and these were characterized by ^1H NMR spectroscopy as $[\text{K}(\text{18-crown-6})\text{SiH}_3\cdot\text{HSiPh}_3]$ (**1b**), in which the SiH_3^- and HSiPh_3 ligands were produced through a ligand redistribution reaction involving PhSiH_3 . The ^1H NMR spectra also revealed the presence of comparable amounts of the hypervalent product $[\text{K}(\text{18-crown-6})\text{Ph}_3\text{SiH}_2]$ (see Supporting Information).¹¹

^1H NMR δ (THF- d_8): **1b** \rightarrow 1.2 (s, $^1J(^{29}\text{Si}-^1\text{H}) = 73.5$ Hz, 3H), 3.5 (s), 5.4 (s, $^1J(^{29}\text{Si}-^1\text{H}) = 200$ Hz), 7.4 (m), 7.7 (m); $[\text{K}(\text{18-crown-6})\text{Ph}_3\text{SiH}_2]$ \rightarrow 3.14 (s), 5.81 (s, $^1J(^{29}\text{Si}-^1\text{H}) = 131$ Hz), 6.8–6.9 (m), 7.98 (d). ^{13}C NMR δ (THF- d_8): **1b** \rightarrow 70.48 (s, CH_2). ^{29}Si NMR δ (THF- d_8): -170.3 (q, $^1J(^{29}\text{Si}-^1\text{H}) = 73.5$ Hz); $[\text{K}(\text{18-crown-6})\text{Ph}_3\text{SiH}_2]$ \rightarrow 68.48 (CH_2), 123.79 (*meta*), 124.31 (*ortho*), 135.25 (*para*), 156.24 (*ipso*). $^{29}\text{Si}\{^1\text{H}\}$ NMR δ (THF- d_8): **1b** \rightarrow -170.3 (s); $[\text{K}(\text{18-crown-6})\text{Ph}_3\text{SiH}_2]$ \rightarrow -73.99 (t, $^1J(^{29}\text{Si}-^1\text{H}) = 131$ Hz).

Crystal Data for **1b** at 115(2) K (CCDC = 821708). $M_r = 594.92$, with $\text{Mo}_{\text{K}\alpha}$ radiation (0.71073 Å); rhombohedral space group $R3m$ (no. 160), $a = b = c = 9.4687(10)$ Å, $\alpha = \beta = \gamma = 98.201(10)$, $V = 820.06(15)$ Å³, $Z = 1$, $2\theta_{\text{max}} = 55.0^\circ$, 1303 unique reflections [$R_{\text{int}} = 0.0540$], $\mu = 0.273$ mm⁻¹, GOF = 1.093, $R1$ ($I > 2\sigma$) = 0.0378, $wR2$ (all data) = 0.0935, Flack parameter = 0.31(7), largest diff. peak and hole 0.408 and -0.562 e Å⁻³.

COMPUTATIONAL DETAILS

Geometry optimizations were performed at the (DFT)–B3LYP/6-311++G(d,p) level of approximation using the Gaussian09 software suite.²⁶ C_{3v} symmetry was imposed for KSiH_3 **2**, while calculation on $[\text{K}(\text{18-crown-6})\text{SiH}_3]$ **1** involved no such constraints. Frequency calculations confirmed that the structures thus obtained were stable minima on their potential energy surfaces, with the exception of the *tet* conformer of **1**, which displayed a low imaginary frequency associated with the tilting of the Si–H bond involved in the inter-ion $\text{Si}-\text{H}\cdots\text{H}-\text{C}$ interactions. The final optimized geometries were then used to obtain wave functions for each system. The topological analysis of the electron distributions and atomic properties were carried out using a combination of the AIM2000 and AIMALL software packages.^{27,28}

The reliability of these calculations was determined through a comparison of the energies, geometries, and electron distributions for *tet* and *inv* structures of **2** at various levels of approximation (see Supporting Information). The B3LYP/6-311++(d,p) calculations were found to provide reasonable values relative to higher level MP2 and CCSD calculations, with the exception of the overall energy difference between the two conformations. However, the calculations consistently converged on the same orientation of the $[\text{SiH}_3]^-$ anion, irrespective of changes in the functional or basis set. Accordingly, all values reported here refer to the B3LYP/6-311++(d,p) calculations (see Supporting Information for details concerning the MP2 and CCSD calculations).

ASSOCIATED CONTENT

S Supporting Information. Details concerning the energies, geometries, and topologies for the B3LYP, MP2, and CCSD calculations at 6-311G(d,p), 6-311++G(d,p), and 6-311++G(3df,pd) level of approximations. We also present the B3LYP/6-311++G(d,p) geometries for the $[\text{K}(\text{18-crown-6})\text{SiH}_3]$ and the experimental geometries for the intermolecular interactions present in $[\text{K}(\text{18-crown-6})\text{SiH}_3\cdot\text{THF}]$ and $[\text{K}(\text{18-crown-6})\text{SiH}_3\cdot\text{HSiPh}_3]$. This material is available free of charge via the Internet at <http://pubs.acs.org>.

AUTHOR INFORMATION

Corresponding Author

*E-mail: dwolsten@unb.ca (D.J.W.), smcgrady@unb.ca (G.S.M.), jon.steed@durham.ac.uk (J.W.S.).

ACKNOWLEDGMENT

We are grateful to the EPSRC (U.K.) and NSERC (Canada) for financial support of this research.

REFERENCES

- Pauling, L. *J. Am. Chem. Soc.* **1932**, *54*, 3570.
- Huhey, J. E.; Keiter, E. A.; Keiter, R. L. *Inorganic Chemistry*, 4th ed.; HarperCollins: New York, 1993.
- Ring, M. A.; Ritter, D. M. *J. Phys. Chem.* **1961**, *65*, 182.
- Weiss, E.; Hencken, G.; Kuehr, H. *Chem. Ber.* **1970**, *103*, 2868.
- Klinkhammer, K. W. *Chem.—Eur. J.* **1997**, *3*, 1418.
- Pritzkow, H.; Lobreyer, T.; Sundermeyer, W.; Hommes, N.J.R.v. E.; Schleyer, P.v.R. *Angew. Chem., Int. Ed. Engl.* **1994**, *33*, 216.
- Schleyer, P.v.R.; Clark, T. *J. Am. Chem. Soc.* **1986**, *108*, 1371.
- Gómez, P. C.; Palafox, M. A.; Pacios, L. F. *J. Phys. Chem. A* **1999**, *103*, 8537.
- Pacios, L. F.; Gálvez, O.; Gómez, P. C. *J. Phys. Chem. A* **2000**, *104*, 7617.
- Prince, P. D. *Structural Aspects of some Group 14 Hydrides and Halides*. Ph.D. Thesis, University of London, London, United Kingdom, 2003.
- Flock, M.; Marschner, C. *Chem.—Eur. J.* **2002**, *8*, 1024.
- Bearpark, M. J.; McGrady, G. S.; Prince, P. D.; Steed, J. W. *J. Am. Chem. Soc.* **2001**, *123*, 7736.
- Bader, R. F. W. *Atoms in Molecules: A Quantum Theory*; Oxford University Press: New York, 1990.
- Sirsch, P.; Clark, N. L. N.; Onut, L.; Burchell, R. P. L.; Decken, A.; McGrady, G. S.; Daoud-Aladine, A.; Gutmann, M. J. *Inorg. Chem.* **2010**, *49*, 11395.
- Wolstenholme, D. J.; Sirsch, P.; Onut, L.; Flogeras, J.; Decken, A.; McGrady, G. S. *Dalton Trans.* **2011**, *40*, 8301.
- Crabtree, R. H.; Sieghhan, P. E. M.; Eisenstein, O.; Rheingold, A. L.; Koetzle, T. F. *Acc. Chem. Res.* **1996**, *29*, 348.
- Campbell, J. P.; Hwang, J.-W.; Young, V. G.; von Dreele, R. B.; Cramer, C. J.; Gladfelter, W. L. *J. Am. Chem. Soc.* **1998**, *120*, 521.
- Aldridge, S.; Downs, A. J.; Tang, C. Y.; Parsons, S.; Clarke, M. C.; Johnstone, R. D. L.; Robertson, H. E.; Rankin, D. W. H.; Wann, D. A. *J. Am. Chem. Soc.* **2009**, *131*, 2231.
- (a) Bondi, A. *J. Phys. Chem.* **1964**, *68*, 441. (b) Nyburg, S. C.; Faerman, C. H. *Acta Crystallogr., Sect. B* **1985**, *41*, 274.
- Lang, P. F.; Smith, B. C. *Dalton Trans.* **2010**, *39*, 7786.
- Wolstenholme, D. J.; Titah, J. T.; Che, F. N.; Traboulsee, K. T.; Flogeras, J.; McGrady, G. S. *J. Am. Chem. Soc.* **2011**, DOI: 10.1021/ja206357a.
- (a) Matta, C. F.; Hernández-Trujillo, J.; Tang, T.-H.; Bader, R. F. W. *Chem.—Eur. J.* **2003**, *9*, 1940. (b) Wolstenholme, D. J.; Cameron, T. S. *J. Phys. Chem. A* **2006**, *110*, 8970. (c) Wolstenholme, D. J.; Matta, C. F.; Cameron, T. S. *J. Phys. Chem. A* **2007**, *111*, 8803. (d) Wolstenholme, D. J.; Cameron, T. S. *Can. J. Chem.* **2007**, *85*, 576.
- Fradera, X.; Austen, M. A.; Bader, R. F. W. *J. Phys. Chem. A* **1999**, *103*, 304.
- Pearson, R. G. *Chemical Hardness*; John Wiley-VCH: Weinheim, Germany, 1997.
- Pearson, R. G. *J. Chem. Sci.* **2005**, *117*, 269.
- Frisch, M. J. et al. *Gaussian 09*, Revision A.02; Gaussian, Inc.: Wallingford, CT, 2009.
- (a) Biegler-König, F. W.; Schönbohm, J. *J. Comput. Chem.* **2000**, *21*, 1040. (b) Biegler-König, F. W.; Schönbohm, J. *J. Comput. Chem.* **2002**, *15*, 1489.
- Keith, T. A. *AIMALL*, version 09.04.23; Gristmill Software: Overland Park, KS, 2009.